International Journal on Recent and Innovation Trends in Computing and Communication
ISSN: 2321-8169 Volume: 11 Issue: 10s
DOI: https://doi.org/10.17762/ijritcc.v11i10s.7633
***Article Received:** 02 June 2023 **Revised:** 28 July 2023 **Accepted:** 12 August 2023*

Statistical Review Evaluation of 5G Antenna Design Models from a Pragmatic Perspective under Multi-Domain Application Scenarios

Manumula Srinubabu[1], Dr. N.V. Rajasekhar[2]
[1]School of Electronics Engineering(SENSE),
VIT-AP University,
Amaravati, A.P, India
e-mail: srinubabu.21phd7112@vitap.ac.in
[2]School of Electronics Engineering(SENSE),
VIT-AP University,
Amaravati, A.P, India
e-mail: rajasekhar.venkata@vitap.ac.in

Abstract— Antenna design for the 5G spectrum requires analysis of contextual frequency bands, design of miniaturization techniques, gain improvement models, polarization techniques, standard radiation pattern designs, metamaterial integration, and substrate selection. Most of these models also vary in terms of qualitative & and quantitative parameters, which include forward gain levels, reverse gain, frequency response, substrate types, antenna shape, feeding levels, etc. Due to such a wide variety in performance, it is ambiguous for researchers to identify the optimum models for their application-specific use cases. This ambiguity results in validating these models on multiple simulation tools, which increases design delays and the cost of deployments. To reduce this ambiguity, a survey of recently proposed antenna design models is discussed in this text. This discussion recommended that polarization optimization and gain maximization are the major impact factors that must be considered while designing antennas. It is also recommended that collocated microstrip slot antennas, fully planar dual-polarized broadband antennas, and real-time deployments of combined slot antenna pairs with wide-band decoupling are very advantageous. Based on this discussion, researchers will be able to identify optimal performance-specific models for different applications. This discussion also compares underlying models in terms of their quantitative parameters, which include forward gain levels, bandwidth, complexity of deployment, scalability, and cost metrics. Upon referring to this comparison, researchers will be able to identify the optimum models for their performance-specific use cases. This review also formulates a novel Antenna Design Rank Metric (ADRM) that combines the evaluated parameters, thereby allowing readers to identify antenna design models that are optimized for multiple parameters and can be used for large-scale 5G communication scenarios.

Keywords- MIMO, Isolation Techniques, 5G Antennas, Sub-6GHz, mm-Wave frequency, Representation, Classification, Correlation, ADRM.

I. INTRODUCTION

Multiband Design of 5G Antennas is a multidomain task that involves frequency pattern analysis, gain optimization, polarization analysis, radiation pattern designs, substrate selection, metamaterial integration, port analysis, packaging optimizations, feed port optimization, and various other factors. There is spectrum available for 5G deployments Both low-frequency and high-frequency ranges (sub-6 GHz and above) and millimetre Wave frequencies. The frequencies 3.3-4.2 Gigga Hertz 4.4–4.9 Gigga Hertz in the sub-6 GHz range band have been deployed in Japan in preparation for the sub-6 GHz band range in the 5G spectrum. Countries such as Europe, the United Kingdom, and Germany utilise 3.4 to 3.8 GHz bands of frequency. while India, as well as China, utilize from 3.3 to 3.6 GHz. Unlicensed 5.15–5.925 GHz frequencies in a sub-6 GHz channel have been proposed as a potential 5G band in several research studies. These studies have been conducted by various academic institutions. Several countries are in the process of putting into operation the 5G spectrum that operates at higher frequencies, such as 24.25 to 27.55 GHz, 26.5 to 27.5 GHz, 26 GHz, 37.6 - 37.6 GHz, and 37.5 -42.5 GHz. A couple of them, such as 3.5 and 26/28GHz, are considered to be pioneer bands [2-3]. There is a chance that 5G will employ frequencies in the range of 53.3 to 66.5 GHz, 55.4-66.6 GHz, 64.8 to 64.8 GHz, and 64.0 to 64.0 GHz [4]. In order for a MIMO system to function properly, its individual antenna parts need to be decoupled from one another.

There are many different decoupling procedures, such as parasitic elements and electromagnetic band gap structures, which may result in a rise in efficiency loss. These ways are used to enhance the isolation between components, and as a result, the complexity. Using various decoupling methods, such as space decoupling, which requires just a little amount of space between

International Journal on Recent and Innovation Trends in Computing and Communication
ISSN: 2321-8169 Volume: 11 Issue: 10s
DOI: https://doi.org/10.17762/ijritcc.v11i10s.7633
***Article Received:** 02 June 2023 **Revised:** 28 July 2023 **Accepted:** 12 August 2023*

the antenna sections, it is possible to incorporate a lower total number of antennas onto mobile terminals. In this work overall size of the antenna array is decreased. MIMO array antennas are provided by references [5] and [6] to handle all of these various difficulties. The construction of antenna arrays allows for the antenna element to be decoupled without the need for a separate decoupling device. This is made possible by the way the array is built. When employing the antenna array described in [5], it was feasible to achieve an isolation level of 17.5 decibels.

The proportion of times in which the efficiency is greater than 62 percent. It's below 0.05 dB in the ECC range (Envelope Correlation Coefficient). Because an isolator with a circular form is included directly into the components of the antenna, there is no need in [6] for an external decoupling structure to be present. The structure was created on a FR4 substrate that measured 50 millimetres by 50 millimetres by 1.6 millimetres. The frequency range that may be used to operate the device is from 3.4 to 3.8 GHz. A measure of antenna diversity is having an ECC that is lower than 0.08. There is a degree of isolation that is lower than -12 dB. In [7], researchers describe the development of ultra-wide band antennas in order to fulfill the enormous data transmission needs of 5G wireless networks. The usage of an antipodal structure that mimics a windmill is one method that may be used to create wideband behaviour. The frequency range of the antenna is between 4 and 10 GHz, and it has a maximum gain of 5 dBi.

It is also upgraded to go from 10 GHz to over 150 GHz with 175 percent of fractional bandwidth; however, the antenna array that utilizes the same structure is not evaluated in the research. This is because it is not relevant to the topic at hand. A 22 MIMO ultra-wideband antenna has a frequency range of 2 GHz to 12 GHz in its frequency range. Included below is the band of operable frequency for 5G that falls below Sub-6 GHz. In way of Compact faculty ground-based two different F structures are built design of antenna array. In order to create a design, a Roger 5880 substrate was used. 143.2 percent of the total bandwidth is fractional, with a maximum gain of 4.8 decibels and less than 20 decibels of mutual coupling. Massive MIMO(mMIMO), is an important method of 5G for expanding channel capacity. A 10-element MIMO antenna array that is designed for usage at 3.45GHz has been created. This array is made up of six monopoles measuring 0.4 in length and four L-shaped slots measuring 0.25 in length. On the substrate, the two different types of antennas are arranged in an alternating pattern[8]. The MIMO antenna array operates at frequencies ranging from 3.3 to 3.6 gigahertz. It was possible to achieve a channel capacity of 48-51 bps/Hz and an isolation level of more than -11 dB [9].

In light of what has been discussed, it is clear that the current models exhibit a wide range of diversity in terms of their performance levels. Because there is such a broad range of performance, it is difficult for researchers to identify the models that are ideal for their use cases and are particular to their applications. Because of this uncertainty, these models have to be validated using a variety of simulation tools, which lengthens the design process and drives up the cost of deployments. The following section will discuss a survey of recently proposed antenna design models, and the following section will compare these models in terms of their quantitative parameters, which will include forward gain levels, bandwidth, complexity of deployment, scalability, and cost metrics. This will help clear up ambiguities that may have been caused by the previous section. Researchers will be able to determine the optimal models for their performance-specific use cases by referring to this comparison and making the necessary adjustments. In Section 3, a novel Antenna Design Rank Metric (ADRM) is formulated. This metric combines the evaluated parameters and enables readers to identify antenna design models that are optimized for multiple parameters and can be used for large-scale 5G communication scenarios. This article draws to a close with some contextual remarks on the models that have been examined, as well as some recommendations for strategies that may be used to better improve their design performance levels for a variety of use scenarios.

II. LITERATURE REVIEW

A wide variety of models are proposed by researchers for designing 5G Antennas, and each of them varies in terms of their internal operating characteristics. A leaky-wave antenna (LWA) with unidirectional beam scanning in millimetre waves (mmW) [1], Fifth-generation new radio (5G-NR) applications, for example, are necessary. A radiating component, a conductive wall, a ground plane, and a partially reflective single-layer surface (PRS) consist of the reported antenna. only one radiating component generates a slanted beam with excellent radiation all over scanning angles to enhance UBS performance. Propagation is impeded by closing a metallic wall used as a reflector to the emitting source. A comprehensive set of design recommendations is revealed by a conceptual model of FPC structures using ray tracing to develop beam-steering abilities versus frequency over predetermined angles. Without changing any parts, the PRS layer scans beams between 24 and 30 GHz and 1045 GHz. Measurement findings show The beam steering ranges from 19° to 54° and spans 24 to 30 GHz, which is consistent with the theoretical analysis. The proposed Fabry-Perot cavity antenna (FPCA) construction is developed. The gain at 24 GHz is 14.5 dBi. The reported antenna could be used in antennas for 5G base stations (BSAs) and mobile communication systems where beam guiding with increased gain & affordable manufacturing process is required for scalability purposes. In the case of a 5G milli-meter (mmW)Wave antenna design, [2] presented a dual-polarized microstrip patch antenna (DPMPA) utilizing FR4. The

International Journal on Recent and Innovation Trends in Computing and Communication
ISSN: 2321-8169 Volume: 11 Issue: 10s
DOI: https://doi.org/10.17762/ijritcc.v11i10s.7633
***Article Received:** 02 June 2023 **Revised:** 28 July 2023 **Accepted:** 12 August 2023*

recommended antenna was created using FR4 PCBs because of their less expensive and easy of design and fabrication. FR4's 5G mmWave electrical properties were also described. To lessen the FR4 substrate loss tangent, an air cavity structure was developed. Patch antenna impedance bandwidth is enhanced by capacitive elements like parasitic patches and L-probe feedings. Dual linear polarization is made possible for MIMO's polarization diversity thanks to the symmetrical antenna radiator and the relative placement of the L-probes. Characteristic mode analysis looked at how well the suggested antenna worked (CMA). The gain of a single antenna was 5 dBi with a bandwidth of 23 to 29 GHz. At a single antenna, cross-polarization suppression was 15-20 dB. For various applications, the 14-antenna array increased gain by 10 and 11 dBi while decreasing cross-polarization by 20 dB.

For 5G MIMO mobile antennas, [3] investigated a Low-Profile Wide-band Four-Corner-Fed Square Patch Antenna (LPW FCF SPA). The proposed antenna has a 2.4 mm low profile and produces four uncorrelated waves with a frequency of 3.3-4.2 GHz using a single square patch (0.03 at 3.75 GHz). For each port, TM 11 half-patch and TM1/2,1/2 quarter-patch are created in order to enable wide-band functioning. TM 11 mode consists half patch is produced when a square patch has two diagonal linear slots. For every port, a square two-edge-shorted quarter-patch is created by shortening the patch's two centerlines. With the half-patch TM 11 mode and the quarter-patch TM 1/2,1/2 modes combined, a wide operating band is made possible. The proposed antenna is detailed, as are the findings from the experiments. For 4G/5G communications, [4] investigated a broadband, wide-beamwidth dual-polarized orthogonal dipole antenna (BWB DPO DA). In order to obtain dual polarization, orthogonal fan-shaped dipoles were used. The use of parasitic components and metal cavities broadened the impedance bandwidth. The metal cavity broadened the antenna's half-power beam widths (HPBWs). An array of 1x4 antennas was built. The gain was more than 0 dBi at 60° pitch angle, the 1.7-3.22 GHz(VSWR 2.0) operating frequency range, E- as well as H-plane HPBWs were greater than 90°. The isolation between input ports in the 1.7-3.22 GHz frequency range was 29 dB levels.

A 5G MIMO antenna with wide performance was presented in [5] as observed from Figure 1, and Figure 2 represents the characteristics of a 5G antenna at Mobile terminals. where initially. For various applications, a Planar Inverted-F Antenna (PIFA) with an inverted T slot is provided.

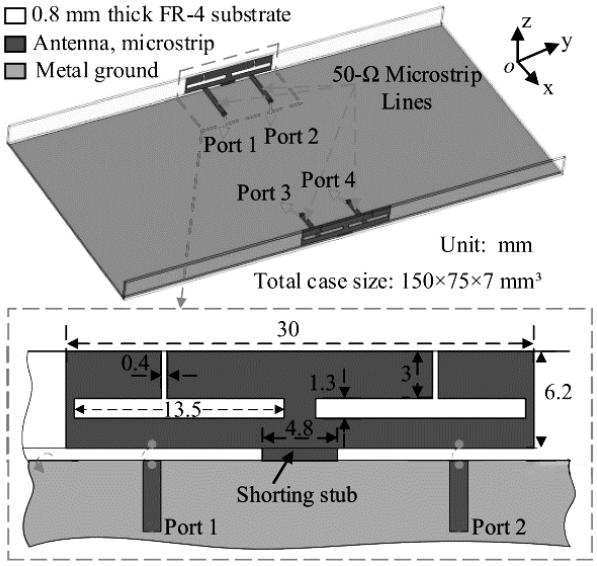

Figure 1. PIFA for 5G sub 6GHz frequency of Mobile terminals [5]

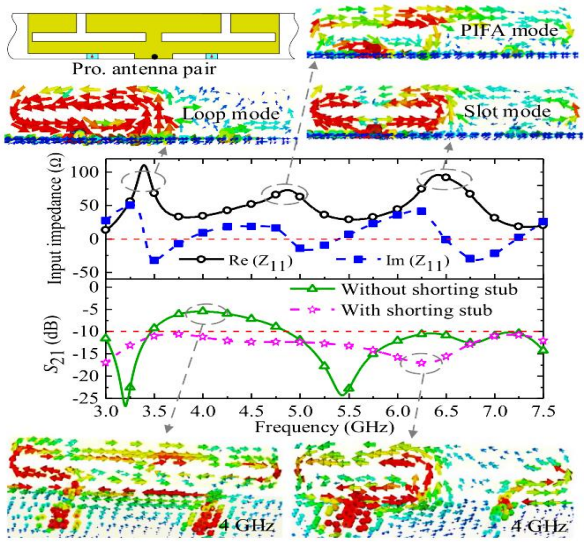

Figure 2. Gain Characteristics of the Antenna with 5G sub 6GHz Frequency of Mobile terminals [5]

The PIFA is expected to have a 78 percent bandwidth thanks to multimode technology. Then, a PIFA-pairs similar bandwidth 2x2 sub-MIMO antenna is created by joining two PIFAs. Over the bandwidth, Dual PIFA isolation is more than 10 dB. 5G NR bands as well as LTE band 46 are covered by a 4x4 MIMO antenna made from two PIFA pairs The effectiveness of the MIMO antenna is shown by simulated and measured data. A dual-band 8x8 MIMO (Multi input and Multi output) antenna for sub-6GHz smartphone applications of 5G technology was presented in [6]. With Orthogonal Pairs of Antennas on the smartphone's Long Sides and Corners (OPA LSC), the design has a totally grounded plane. To minimize mutual contact at both bands, an 8.2 mm short neutral line joins orthogonal pairings. Each antenna element is a folded monopole with a 17.85x5 mm2

International Journal on Recent and Innovation Trends in Computing and Communication
ISSN: 2321-8169 Volume: 11 Issue: 10s
DOI: https://doi.org/10.17762/ijritcc.v11i10s.7633
***Article Received:** 02 June 2023 **Revised:** 28 July 2023 **Accepted:** 12 August 2023*

size that works between the frequencies of 4800 and 6000 MHz. High ECC, MEG, overall efficiency, and channel capacity are features of the prototype antenna. User effects on the antenna and low peak SAR are also shown. Work in [7] created a low-SAR, 4-MIMO antenna array implemented in For 5G mobile terminals, TCM (theory characteristic modes) consists of PEC and dielectric lossy based on handset design applications.MIMO array is constructed and tested at the end. 3.4–3.6 GHz is covered by a 10 dB impedance bandwidth. Isolation levels greater than 15.4 dB divide antenna components. Their productivity ranges from 81.3 to 89.9 percent. ECC is less than 0.07. At 10 g, Four antennas produce 0.47 W/kg of SAR at the same time. The suggested MIMO antenna array has an acceptable efficiency, isolation, and ECC with the lowest peak SAR. This article demonstrates how to make low-SAR mobile phone antennas. While work in [8] presented a dual-broadband dual-polarized ME-dipole antenna (DBDP MEDA) with a common aperture for 5G applications.The antenna operates at 2.35-3.93 GHz and 24-34 GHz, with dual-polarized photons and a similar aperture in both bands. The proposed antenna may produce dual-polarized, two-dimensional (2-D) more no. of beams in the millimetre(mm)wave range. Two ME dipoles make up the antenna. For high-gain 2-D switching with dual polarization in the MM-wave band, four horn antennas with inclined inner walls are excited by a ME-dipole supplied by a substrate-integrated waveguide (SIW). Four horn antennas are combined into a large dual-polarized ME-dipole antenna for the lower frequency range. The design and functioning of the antenna are shown. A 33.9 percent (24-33.91 GHz) and a 50.3 percent (2.35-3.93 GHz) impedance bandwidth is what was discovered. The greatest gains of the proposed antenna are 10.67 (3.8 GHz) and 14.85. (32.2 GHz). The antenna has a consistent pattern and a wide impedance spectrum, covering the majority of 5G microwave and MM-wave frequencies, thanks to the robust ME-dipole and horn antennas.

Work in [9] provided instructions on how to use SIW technology will be used to create a phased antenna array for 5G base stations. Sector Illumination is constant due to the array's vertical cosecant radiation pattern. The array features There are 16 SIW travelling wave subarrays with 12 slot-coupled MSA each, as well as phasing elements for cosecant-shaped radiation. A potential 5G mm-wave spectrum, the Array is Implemented to operate at 28 GHz with more than 10% BW. Excellent active impedance and +/60° azimuth scanning are features of the phased antenna array. The array design is successful in experiments. To meet the extra frequency range and 44 MIMO prerequisites of 5G, a tri-band MPA and its 4 modules are preferred [10]. The first three independently tuneable modes are based on a Half-Mode Microstrip Patch (HMMP) and cover the three Chinese 5G bands. The suggested triple-band MPA equalises antenna volume and impedance bandwidths with impedance bandwidths of -6dB at 2.47-2.75 GHz, 3.39-3.60 GHz, and 4.69-5.10 GHz. This module is consisting of four identical patches that are rotated one after the other. The module performs quite well for different scenarios.

Research in [11] developed a Poor MIMO antenna array for 5G smart phones based on characteristic modes (TCMs). TCM looks at a geometrically symmetric dipole antenna first. Symmetric and Reverse Modal (SRM) currents are used by low-SAR antenna components. The MIMO array is then formed by eight antenna parts. The proposed MIMO array has a 6 dB impedance bandwidth between 3.4 and 3.6 GHz. Antenna component isolation is more than 16 dB. While work in [12] conducted research on Miniature Dual-Polarized Base-Station Antennas (MDP BSA). The wavelength of the element (which is the core working frequency) is high for different scenarios. The cross-coupling slot of the antenna has four vertical slots, which enhance high-frequency suppression. The C-slots on Gnd1 reduce axial cross-polarization. The antenna's operational bandwidth is 25.6%, and its cross-polarization ratio is 22 dB. The design is tested using a 13-linear array. At 3.3–4.0 GHz, the array's average gain is 11 dBi. The array features broad harmonic suppression and good out-of-band rejection up to 9 GHz.

For 5G MIMO metal-rimmed smartphones, [13] presented a pair of orthogonal-mode wideband dual-antennas with a shared radiator. Wideband decoupling is accomplished by combining In the lower band, There are orthogonal monopole/dipole modes, as well as orthogonal slot/open-slot modes in the upper band. The dual-antenna pair uses an orthogonal-mode design (OMD) to provide significantly greater than 21.0 dB isolation across the whole frequency range without the use of extra decoupling devices. The impedance bandwidth is wide, ranging from 3.3 to 5.0 GHz. An 8x8 MIMO is created by attaching four dual-antenna pairs to the smartphone terminal. The proposed 8x8 MIMO system may provide 12.0 dB isolation and a 0.11 envelope correlation coefficient across all ports, according to simulation and experimental results. The average efficiency for a dual-antenna pair is 74.7 percent and 57.8 percent. The proposed design may be used in upcoming 5G devices because of its shared radiator, high bandwidth, and metal rim compatibility. Work in [14] discussed a Scalable Wideband Phased Modules Array (SWP MA) that covers 5G frequency bands that may be incorporated into a multi-layered organic packaging with integrated antennas (24.25-29.5 GHz). The package includes a ball-grid array, RF, IF, DC, and digital interconnects to support RFICs, filters, and combiners, and an array of 88 dual-polarized antenna components with 5.1-mm spacing (BGA). Its form factor is tiny, measuring 42.5 mm x 42.5 mm x 1.65 mm. By incorporating a novel ME dipole antenna in the device, the design provides wideband operation at a low cost or complexity (e.g., air cavities or extra substrates). With >6GHz BW and 0-5 dBi gain, 2 different prototype antenna

International Journal on Recent and Innovation Trends in Computing and Communication
ISSN: 2321-8169 Volume: 11 Issue: 10s
DOI: https://doi.org/10.17762/ijritcc.v11i10s.7633
***Article Received:** 02 June 2023 **Revised:** 28 July 2023 **Accepted:** 12 August 2023*

array packages include three different antenna types. Additionally tested are bandpass filters and power combiners based on LC polymers.

Researcher proposed a metal-framed MIMO antenna array for 5G NR smart phones.[15]. An 8x8 MIMO antenna arrays are developed by implanting 8 identical antennas (Antenna1 to Antenna8) into the mobile phone's metal chassis. Each antenna element is a slot antenna with a 50 ohms feedline and an open slot in the form of an L. To guarantee perfect impedance matching in the higher frequency range, a Tuning Stub (TS) may be utilized. The proposed eight-antenna array can support WLAN 5 GHz and 5G NR Bands. Additionally, antenna efficiency ranges from 50 to 82 percent and envelope correlation (ECC) value from 0.11, the elements of the array next to it are isolated by more than 12 dB. At a signal-to-noise ratio of 20 dB, the suggested design of 8 antenna array is the highest channel capacity of 43.93 b/s/Hz. A Dual-Band, Dual-Polarized Filtering Antenna (DBDP FA) with higher selectivity was reported in [16]. By Etching or removing 4 slots on each side of a square radiating patch, two working bands and a natural radiation null are created. Two additional radiation nulls are produced by an open-circuit stepped-impedance resonator on a microstrip line (OCSIRs). The realised gain thus includes a dual-band bandpass filter. The port isolation is 37 dB, and each antenna is differently supplied. By creating and testing a prototype antenna element and 14-arrays, our idea is confirmed. The antenna element has a VSWR of 1.5 and operates at 3.28-3.71 and 4.8-5.18 GHz. 17.7 dB of out-of-band gain suppression is achieved. For a 5G base Stations operating at sub-6 GHz, the recommended antenna performs well.

An array of dual-band &dual-polarized millimetre-wave patch antennas (DBDP MWPA) with excellent beam scanning and mutual coupling was suggested in [17]. The recommended antenna array delivers a significant increase in low- and high-band bandwidth via the use of capacitive feed and layered design with additional parasitic strips. The array's footprint is minimized, and At 26 GHz, the component distance is less than 0.36 wavelength, improving beam scanning efficiency in both bands. Due to their close proximity, two efficient decoupling techniques are applied to enhance the isolation between array components. A number of newly released industrial mm-Wave antenna technologies are larger than the specified antenna array, which measures just 18.2x4.1x1.07mm3.According to our simulation, the antenna elements can simultaneously cover 5G frequency ranges. The four-element array simultaneously scans the low-band beam at 60° and the high-band beam at 45°. The array is an excellent choice for 5G mm-Wave technology since its experimental S11 parameter, MC-mutual coupling, and radiation patterns match the anticipated results. In order to support 5G-NR applications, [18] presented a Shared Aperture Planar Quasi-Yagi Antenna (SAP QYA) with a wide range of complementary pattern (polarisation) diversity Even-odd mode feedings suggest a small shared aperture antenna with good port isolation. Surface current distribution is used to analyze the special pattern reconfigurable technique while to adding the monopole mode & dipole mode. Controlling the monopole and dipole feeding states results in a pattern-reconfigurable Yagi antenna with 4 modes (i.e.omnidirectional, broadside, and two slanted). The quasi-Yagi antenna with the dimensions of 0.5110 x0.2440x0.0050(measured in free space wavelength and frequency) is built and tested. The 10 dB BW of the 4 modes covers the 5G-N78 spectrum at 3.3-3.8 GHz (14.1 percent). The maximum efficiency of radiation is 80%. The proposed miniature antenna is ideal for 5G-NR communication because of its low cost, straightforward construction, high bandwidth, superior radiation characteristics, and pattern/polarization re-configurability.

Work in [19] offered The antenna-in-package (AiP) solution for mobile terminals is used in the development of innovative 5G mm-wave antenna designs that incorporate non-mm-wave methods. The unique Implementation includes mm-Wave antennas-in-package integrating and as non-mm-Wave antennas (AiPiA), mm-Wave antennas-in-package as non-mm-Wave antennas (AiPaA), and others (AiPiaA). In comparison to traditional AiP-based mm-Wave antenna designs, this approach achieves total solutions for 5G cellular communications antennas to cellular phones, which benefits mobile telephone antenna designers, antenna space in mobile telephones, and 5G antenna applications for cellular phones. For 5G MIMO access-point applications, [20] examined the design of a four-Port annular-ring (FPAR) patch antenna that produces four decoupled waves in the 3.3–5.0 GHz range (41 percent at 4.15 GHz), with efficiency greater than of 84 percent & less than 0.05 of ECCs. The four ports of the AR patch, which is ten millimetres above the ground plane, are uniformly spaced out by 90 degrees (0, 90, 180, and 270). There is an impedance-matching ring gap in each port. 4 gap-coupled shorting (GCS) strips are implanted to short-circuit the patch to the ground plane at 45°, 135°, 225°, and 315° angles. GCS strip is separated to two nearby ports. Between 3.3 and 5.0 GHz, the 4 ports may produce decoupled waves with low ECCs. Port isolation levels are increased via a design expansion process.

Scientists developed a wideband circular polarization planar array antenna for 5G mm-wave applications (WCP PAA) in [21]. The antenna component is fed through a slot in the substrate-integrated waveguide (SIW), allowing for simple integration. Its broadband CP polarizers are two semi - circle patches and two copper poles suspended from the ceiling. The antenna's 3 dB AR BW is increased by four CP modes by combining the patch, post, and slot. The design and functioning of the antenna are shown. The modelled antenna element has a 7.25 1 dBic gain over the frequency spectrum, a 41.28 percent

International Journal on Recent and Innovation Trends in Computing and Communication
ISSN: 2321-8169 Volume: 11 Issue: 10s
DOI: https://doi.org/10.17762/ijritcc.v11i10s.7633
***Article Received:** 02 June 2023 **Revised:** 28 July 2023 **Accepted:** 12 August 2023*

AR BW from 25.66- 39.01 GHz, and a 44.62 percent impedance BW from 24.41 to 38.43 GHz. Most 5G mm-wave frequencies are covered by The wide AR/impedance overlapping antenna bandwidth (25.66-38.43 GHz). A planar 4x4 antenna array fed by a completely integrated SIW network is designed, built, and evaluated to increase antenna gain for practical applications. The array has an impedance BW of 40.21 percent between 24.42 and 36.71 GHz, a 36.51 percent AR bandwidth between 25.3 and 36.6 GHz, and a peak gain of 19 dBic. The proposed antenna has a novel broadband CP operating concept, a low profile, and superior radiation effectiveness for 5G mm-wave applications.

Work in [22] creates in WISAP stands for wideband integrated slot antenna pair, and it recommends a wide-band decoupling technique to prevent severe coupling among two closely spaced open-slot antennas. In order to eliminate considerable mutual coupling, Two evenly spaced open-slot antennas can be connected to form a top slot structure with odd & even-mode resonant frequency in the lower and upper bands. To boost BW, the top slot may boost the antenna pair's effective radiation aperture. In that recommended slot antenna pair exhibits good impedance matching, isolation, and diversity across the between frequencies of 3.3-5.0 GHz and has a footprint of 28x7x1.8 mm3. Following are steps for simulating, creating, and measuring an 8 by 8 Four sets of slot antenna pairs are employed in a MIMO system. The 8x8 MIMO system may produce isolations of 10.8 dB According to simulated and measured results ECCs of less than 0.14 of frequency range 3.3-5.0 GHz.Ant1 & Ant2 efficiency values are 55.0% and 83.1%, and 52.5% and 83.1%, respectively. The recommended solution provides wide bandwidth, a compact footprint, a high degree of integration, and compatibility with metal rims. While work in [23] investigated a high-gain superstrate antenna array (HG SAA) operating at 60 GHz. The proposed antenna array is affordable and effective. Millimetre-wave/5G transceivers only incorporate the specified structure. The relative bandwidth is 10.7 percent, the array boresight gain is 19.4 dBi, and the maximum gain fluctuation is 1.7 dB.

For prospective applications such as smart wearables, radars in vehicles, and remote-based devices in smart 5G applications, Ni-based EMM nanotechnology [24] is used to create small, transparent, and flexible 5G MIMO and mm-Wave array antennas. EMM is clear, stable, and extremely conductive. To boost transparency and radiation efficiency, EMM structures are implemented & studied. An EMM-based 5G MIMO antenna runs in a 5G n79 band and has an ECC of 0.005, 93 percent transparency, 85 percent radiation efficiency, and 20 dB of isolation (4.4-5 GHz). Findings from simulations and measurements agree well. In the 26 and 28 GHz channels, clear and able-to-adapt 5G mm-Wave arrays with a peak gain of 9.6 dBi are shown. A low-cost, highly effective, RA antenna made entirely of metal with mechanical beam steering was presented in [25]. A copper cylinder with a cuboid-shaped notch is the recommended unit cell (UC) for acquiring a 1-bit reflective zero phased for normal incidence of TE & TM Mode waves. The proposed UCs are able to construct a 2-D beam-steerable RA antenna. By rotating the UCs, RA antennas with six different beam orientations are shown as examples. From 22 to 33 GHz, the RA antenna's impedance matches are all less than -10 dB, and its observed radiation patterns correspond to the predicted equivalents in six different beam direction scenarios. The RA antenna with broadside radiation patterns has an 18.9 dB peak gain and a 1.5 dB gain drop from 24.7 to 30 GHz. The recommended UCs are all-metal with no active RF Antenna elements and insulating substrates, which contribute to the proposed RA antenna's good overall efficiency.

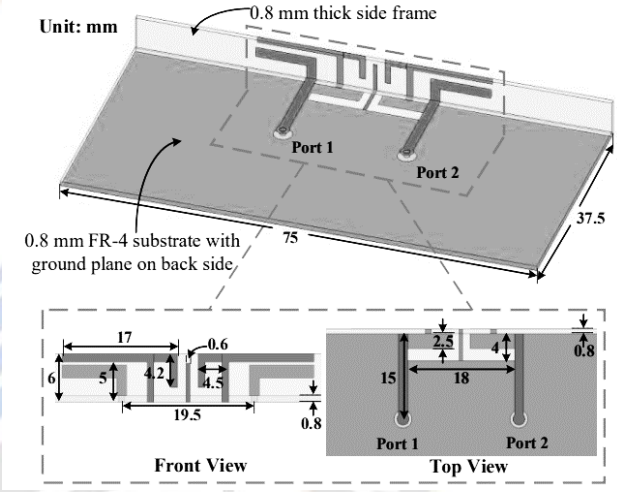

Figure 3 (a). Wideband decoupled dual-antenna pair (WDDAP) for gain and bandwidth enhancement of MIMO based-sub 6 GHz frequency [27]

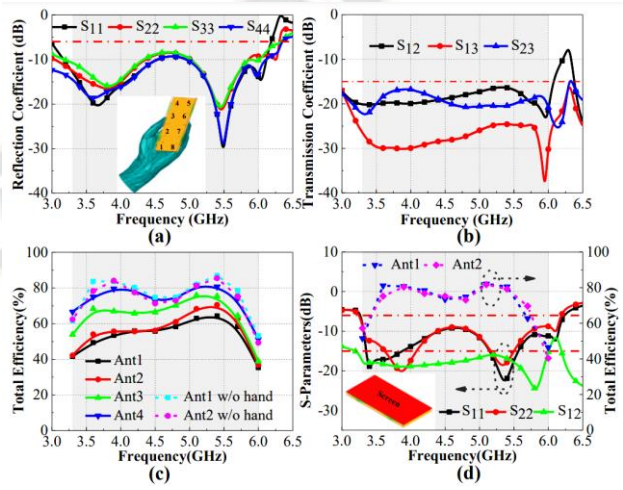

Figure 3 (b). Frequency response for different metamaterial types [27]

Due to its less in cost , good efficiency, and capable high power, the proposed RA antenna is a viable choice for 5G millimetre-wave applications. Figure 3 (a). Wideband decoupled dual-

International Journal on Recent and Innovation Trends in Computing and Communication
ISSN: 2321-8169 Volume: 11 Issue: 10s
DOI: https://doi.org/10.17762/ijritcc.v11i10s.7633
***Article Received:** 02 June 2023 **Revised:** 28 July 2023 **Accepted:** 12 August 2023*

antenna pair (WDDAP) for gain and bandwidth enhancement of MIMO based-sub 6 GHz frequency [27]

Research done in [26] proposes a common-aperture (CA) 5G antenna design for integrated wireless devices that are small and compact. Verification of an integrated antenna design using a dipole and tapered slots 3.6 GHz in sub-6 GHz and 28 GHz in mm-wave. The 3.6 GHz dipole that is the foundation of the antenna's design is supplied by a tapered slot and microstrip line balun. The tapered slot antenna stimulates the dipole at 3.6 GHz, and at 28 GHz, it serves as an antenna. Unique design provides a high-frequency ratio by using a single optimized feeder for both structures.

The dipole is dual-functional in that its arms act as antenna footprints for mm-wave arrays to two tapered slots. The mm-wave arrays' main beams and the tapered slot antenna's main beams are distinct. This arrangement spans a 120° -direction. A 75x25x0.254 mm3 Rogers RO-5880 prototype is created as a proof of concept. Measurements and simulations demonstrate the viability of the idea. While, work in [27] investigated a wideband decoupled dual-antenna pair (WD DAP) as observed from Figure 3 (a), for 5G mobile terminals using characteristic mode theory. Broadband and high isolation are achieved through parasitic strip and weak ground structure. An eight-element MIMO antenna is made up of four pairs of decoupled antennas that are mounted on each side frame. In order to reduce mutual antenna coupling, slits are etched into the system ground. The suggested 8- MIMO antenna can cover the 5 GHz wireless LAN as observed from Figure 3 (b) and 5G New Radio frequencies, according to simulation and testing results. Any two ports may be isolated by 15 dB.

For 5G mmW applications with a wide bandwidth, [28] investigated an end-fire Each antenna in this array is a Substrate-Integrated Waveguide (SIW) H-plane horn for vertical polarisation and a microstrip-fed dipole for horizontal polarisation. The horn antenna aperture has two metal vias added for vertical polarization. Each horn's apertures partially overlap to form a four-component antenna array. A multilayer PCB prototype was created. For both polarizations, the impedance bandwidth ranges from 24.4 to 29.5 GHz. measured results are consistent with models. With a scanning angle between 34° and 33° and less than a 3 dB gain loss, 9.16 and 9.27 dBi are the maximum gains for vertical and horizontal polarizations, respectively. The proposed antenna has promise for antenna-in-package or 5G mmW mobile phones. In the LTE42 frequency band, [29] proposed a 10-element self-isolated antenna array (SIT EAA) for 5G mMIMO mobile terminal applications. The suggested antenna parts are organised in a two - dimensional array along the long sides of the mobile chassis. Half-wavelength shorted loop antennas, which are seldom utilized because of their size in comparison to quarter-wavelength antenna designs, are the kind of antenna construction that is advised. It has a footprint of (where 14.3 /13.2 is the 3.5 GHz free space wavelength) and is a printed, shorted, tiny loop antenna. A short capacitive strip in the form of a flag is used to excite the suggested loop antenna. By creating an internal loop through inward meandering, compactness is increased. The position and size of this loop modify the matching level and resonance frequency at 3.5 GHz. Impedance matching is better than -10 dB according to theoretical, simulated, and measured results, and overall efficiency is higher than 65 percent for the 3.5 GHz frequency range (3.4-3.6 GHz). The best MIMO and diversity performance (lower than 0.055) and the maximum channel capacity (approximately 54.3bps/Hz) of comparable systems are incorporated into a 10x10 MIMO system. The proposed antenna design complied with the results of the SAR simulation. The recommended ten-element MIMO antenna is perfect for 5G smartphone applications operating below 6 GHz.

Work in [30] used a Layered Pane of Glass (LPG) for a vehicle that included a periodic patch director and printed 5G monopole antennas. Since the suggested monopole antenna is printed on laminated window glass, no extra mounting space is required. The monopole's rectangular disk improves bore sight. Optimal array spacing on periodic patch director elements increases gain. The suggested antenna is constructed and put through its paces in a completely anechoic room to confirm its efficacy. The findings show that the suggested periodic patch director and monopole antenna are appropriate for mobile devices operating in 5G bands. A single-input switching beam antenna for 5G millimetre-wave networks was created by researchers [31]. The main beam is electrically switched in two directions by the implemented microstrip-line-to-slot line single-pole dual-throw (MLSL SPDT) switch, which is based on readily accessible p-i-n diodes. The antenna is constructed on CuClad using a lower-cost PCB technique. Numerical models and observations from anechoic chambers agree well. With a 3 dBi gain and an 80° beamwidth in both modes, the antenna can horizontally flip the main beam between +45° and -45°. The provided prototype has a straightforward small footprint, an inexpensive fabrication method, a low profile, and an electrical switching mechanism. The antenna is suitable for less expensive millimetre-wave 5th Generation applications thanks to these characteristics, notably in Internet-of-Things end devices.

For 2, 3 and 4Generation and sub-6 GHz 5Generation systems, [32] proposed a dual-band, dual-polarized base station antenna with a notch band (DBDP NB). The antenna is composed of a crossed Y-shaped balun, a two-layer parasitic annular disk, and a four-leaf loop radiator. Each radiator is given a mouse-ear-shaped arm to enable dual-band operation and a 2.9-3.2 GHz notch band. Enhancing the bandwidth are rings and gradient strips. According to the measured results, the recommended antenna has an isolation of more than 30 dB, a VSWR of 1.7, and fractional bandwidths of 55.8 percent (1.55-

International Journal on Recent and Innovation Trends in Computing and Communication
ISSN: 2321-8169 Volume: 11 Issue: 10s
DOI: https://doi.org/10.17762/ijritcc.v11i10s.7633
***Article Received:** 02 June 2023 **Revised:** 28 July 2023 **Accepted:** 12 August 2023*

2.75 GHz) and 14 percent (3.3-3.8 GHz). During working bands, this design produces 7.1 0.5 dB gain and 68 5° HPBW. It may be used for sub-6 GHz 5G base station applications as well as 2G, 3G, and 4G networks. The design of mmWave 5G tablet antenna modules was covered in [33]. The antenna module comprises two four-chain end-fire arrays (TFC EFA) and one eight-chain broadside array. Broadside patch antennas have two polarizations and are air-filled. The suggested antenna allows for a flexible dielectric cover design, which could enhance performance. In a unique surface-mountable chip antenna, a vertical polarised end-fire antenna is accomplished on a low-profile substrate. It is possible to create a dual-polarized end-fire antenna by collinearly combining a horizontally polarised mesh grid antenna with a V-pol. chip antenna. A tablet's polycarbonate case has been altered to improve end-fire antenna performance. Utilizing the cumulative distribution function (CDF) of effective isotropic radiated power (EIRP), the 5G standard developed by the 3GPP measures spherical coverage. Spherical coverages are provided by variations in the plastic cover, blocking, and no. of mm-Wave 5G communication modules.

Work in [34] investigated creating an integrated 4G/5G antenna using a square ground slot with an open end (SGS OE). The proposed configuration makes use of the 4G module's antenna footprint for 5G. The rectangular slot, which runs at 800 MHz and 2 GHz, is now equipped with a four-element Vivaldi antenna operating at 28 GHz. This array has an end-fire gain of 11 dBi. A 150x75x0.51 mm3 RO-5880 prototype is created for design validation. The design features a wide mm-wave frequency range (26 to 32 GHz) with S11 less than -7dB, as well as two low-frequency bands (1.9 to 2.6 GHz and 770 to 810 MHz) with less than S11 parameter is -6dB. Diversity-validated to MIMO antenna configurations. Similarly, a broadband, small-footprint planar Yagi antenna (BSF PY) in-package proposal for 5G wireless communications was presented in [35]. Monopole taper radiators are used in the recommended Yagi antenna design to enhance bandwidth, decrease size, and make feeding easier. The proposed AiP is capable of simultaneously using all three 5G New Radio frequencies. The circuit is constructed utilizing a low-loss polymer covering and a high-precision, high-resolution glass packing approach. With a fractional bandwidth of 49 percent, the operational spectrum ranges from 24.25 to 40 GHz. 3.05 mm x 5.56 mm constitutes an antenna element (0.25-0.45-0-0). The gain is more than 4 dBi, and the band-wide S 11 is less than -10 dB. The recommended element has a wide band gain of 6.2 dBi in a two-by-one array. The recommended AiP design is small and capable of using all 5G bands. While addressing 5G concerns including mm-wave route loss and transmission loss, it can be applied to vast arrays and easily included in the packaging to create compact system-in-package applications.

A dual-polarized, fully planar radiating device with embedded coupled dipoles (DPFP RD ECD) was reported in [36]. These components enable three distinct objectives: first, an Enlarging required BW with a drop in antenna size compared to the rest of topologies; second, a secondary lobes minimization; and third, an enlarging the bandwidth at lower frequency band i.e. 1.69 GHz to 1.427 GHz. Two sets of planar dipoles are used in the dual-polarized broadband antenna that is presented. Future 5G needs in the microwave region will be met by this research's development of an antenna with return losses under -14 dB and cross-polar isolation above 28 dB. Similarly, work in [37] evaluated the design of a low-profile, wideband vertically polarized antenna with monopole-like radiation characteristics (LP WVP MR). This antenna, like a typical mono-cone, has internal matching and reactive load. Mono-cone structure with crossed substrates reduces antenna weight and increases design flexibility. Using triangular patches that are capacitive coupled and shorting pins, the antenna profile's height is decreased. The minimum operational frequency's free-space wavelength is known as min. Impedance is changed by an inter-digital capacitor near the antenna's input. The suggested antenna emits light in omnidirectional patterns that are constant and monopole-like. Voltage standing-wave ratio (VSWR) of 2.2 with impedance bandwidth of 81 percent from 1.66 to 3.95 GHz, concurrently spanning the 3.3-3.8 GHz 5G N78 range and the 1.7-2.7 GHz 4G LTE band. The recommended antenna is for tiny base stations installed in interior ceilings.

For 5G base stations, [38] suggests using a triple-band shared-aperture dual-polarized antenna array (TB SA DPA). A low-band (LB) antenna operating between 0.69 and 0.96 GHz, a middle-band (MB) antenna array operating between 1.8 and 2.7 GHz, and a high-band (HB) antenna array make up the shared-aperture antenna array. The wideband band stop eliminates the LB antenna's influence on the frequency-selective surface of the MB/HB array (FSS). The MB antenna, which was installed The co-design with the wideband band pass FSS has no effect on the HB antenna array's radiation performance. Within a volume of 0.69L x 0.69L x 0.177L, the LB antenna, MB antenna array, and HB antenna array are all effectively integrated. (L denotes the wavelength of free space at 0.69 GHz.) The proposed low-profile shared-aperture antenna array has average gains of 6.5, 7.6, and 8.2 dBi for LB, MB, and HB, respectively. Massive 5G massive MIMO allows for wide bandwidth, low profile and height, shared aperture, and compact antenna arrays. Work in [39] proposed a concept for 4x4 5G MIMO functioning in the 3.3-4.2 GHz band by forming a cross with 4 GCPW-fed open-slot antennas. With four wide operational bands (almost 24 percent centred at 3.75 GHz) and antenna efficiency more than 40 percent, The 4 conjoined slot patch antennas have a 1 mm low profile (approximately 0.01 at 3.3 GHz) and a 42 mmX42mm compact size (0.46 dB at 3.3 GHz).The bandwidth and decoupling of the four slot antennas are enhanced by the linked circular slot. Conjoined slot antennas can be placed in the 5G

International Journal on Recent and Innovation Trends in Computing and Communication
ISSN: 2321-8169 Volume: 11 Issue: 10s
DOI: https://doi.org/10.17762/ijritcc.v11i10s.7633
***Article Received:** 02 June 2023 **Revised:** 28 July 2023 **Accepted:** 12 August 2023*

terminal's dielectric back cover to their 1 mm low profile, which lowers antenna volume under real-time scenarios.

On an individual user equipment size ground plane, 3 distinct microstrip slot radiators are used (UE SGS) were the subject of research in [40], enabling the user to use a number of usable bands as observed from figure 4, esser cellular bands, Sub-6 GHz FR-1 bands, and mm-wave 5G bands are all included. Figure 4. Design of 8-line gain and bandwidth enhancement Antenna of MIMO based-sub 6Ghz frequency [40]

First, a 2-port Type-I MIMO antenna with polarization diversity and a 4 dBi gain is constructed for cellular bands between 1.6 and 2.2 GHz and 2.5 and 2.7 GHz. The sub-6 GHz fifth generation frequency range from 3.3 to 5 GHz is 7 dBi gain is achieved using two 2-port MIMO antennas Design I.e. type - II antenna model new connected meander ground slot, decoupling is accomplished. Third, for the 5G spectrum from 27-29GHz (|S11|; -10dB), two circularly polarised 1x8 linear arrays (Type-III) with neighbouring port isolation of 20 dB and realised gain of 12dBic are proposed. The proposed phased array makes use of a 5G analog beam former built on SiGe. Beam steering on the array axis is 30°. The performance of the prototype is further distinguished by extra metallic parts, hand, and head phantom. The prototype is a suitable choice for the next UEs due to its successful simulation and experimentation.

Suggests a dual-band multimode high-gain stacked-patch antenna (DB MM HG SPA) based on SISL[41] applications of the fifth generation. The suggested antenna consists of 10 metal layers with air holes and five FR4 dielectric substrate layers. The driven patch produces the TM 10 and TM 02 modes, while the horizontal slot and U-slot carry out dual-band. U-slot stacked patch in the high-frequency band to increase the gain, reduce suppression gain in out-of-band frequency, and suppress the TM 02 mode radiation pattern split. This hypothesis is confirmed by fabricating and measuring the antenna. The recommended antenna operates at frequencies encompassing the 5G range, 3.21-3.66 and 4.75-5.40 GHz, and the observed and projected results show good agreement. a very effective antenna. 9.12 and 8.65 dBi are the band gains. Similarly, work in [42] asserts that integrating mobile device components necessitates a reduction in antenna size.

A vertically stacked dipole array working at 28/38 GHz is described in this paper. The recommended dual-band small antenna (DBSA) has a large bandwidth. A 28 GHz band patch in the intermediate plane, as well as symmetric 38 GHz band radiators above and beneath a multilayer substrate, comprise the dual-band antenna configuration. We define two kinds of antenna constructions, one with a differential feed topology and the other with a single-ended feed topology,10 dB of bandwidth, 23.9 and 14.4% return loss, and 4.8 and 4.6 dBi gain at 28 and 38.5 GHz are all characteristics of the single antenna. The antenna array has a gain of 9.0 dBi at 28 GHz and 10.3 dBi at 38.5 GHz. Due to its flexibility flexible, It is bendable and can be inserted into the terminal's side. For millimeter wave 5G communication, it must have a sufficient gain, wideband, dual-band, and compact size.

A DPA EFR stands wideband compact dual-polarized antenna pattern was reported in [43] for use in mm-wave applications. S11 bandwidth of -10 dB (25-29.5 GHz). The antenna has a 3.4mm width and a 1.6mm thickness. In H-mode and V-mode, the four-element array achieves 9.9 and 9.1 dBi, respectively. The antenna has powerful H-mode and V-mode scanning and a broad beam width in elevation and azimuth. While for 5G base stations, [44] provided a small, inexpensive, low-profile, suspended patch antenna with dual polarization (SPA DP). The suggested antenna features a vertical metal wall, modified L-probe feeds, a parasitic patch, and radiating and radiating patches. Two capacitive feeds power the main patch, allowing for dual (45° slant) polarization. Ports are enclosed by vertical metal walls. The parasitic patch enhances port isolation and Matching input impedance (S11, S22) (S21). The prototyped antenna has an impedance bandwidth of -10 dB and |S11 | and |S22 | ratios of 45 and 36%, respectively. In the required frequency range, port isolation is -30 dB. E/H-planes provide symmetric radiation patterns with steady beam widths of 56°–65°. Antenna gain of 8.95 dBi. It describes calculations and experiments.

Work in [45] demonstrated a miniaturized antenna in package (AiP) with broadside & end-fire arrays and dual 28/39 GHz bands for 5G millimetre-wave handsets (MAP BEFA). The 5.8mm19mm1.122 mm AiP is shown on this page. With a 10 dBi antenna gain, 3 GHz return-loss bandwidth, and greater than 10 dB isolation for broadside & end-fire arrays, with 5G AiP being the smallest. The 14-patch antenna array used by AiP is for end-fire and broadside radiation and the patch antenna size is reduced by components, In between the patch layer and the ground plane is a multilayer RIS. In 5G PCB-stacked antennas, where each layer necessitates copper space, this layered RIS design works well. A highly connected T-shaped side through a wall is added to the end-fire array antenna to reduce its size and boost its bandwidth. The AiP offers a 10 dB RL(Return-Loss) BW of 35.18 to 41.00 GHz for VBFDA & 26.22- 29.57 GHz for Multilayer RIS Patch Antenna (MLRPA). Antennas with MLRPA and VBFDA both produce 11.6 dBi. Work in [46] suggested a Y-shape topology made up of three wideband MPAs (YTTW MPA) for 5G access point MIMO operation in the 3300-4200 MHz range Each MPA has a 22-mm top-patch length and a 10 mm antenna height (or around 0.11 at 3300 MHz). A feed strip at the top-patch centre capacitively activates each MPA, and two shorting strips connect it to the ground plane. The open end of the top patch has one shorting strip, and a Y-shaped structure that all three MPAs share has the other. Three tiny

International Journal on Recent and Innovation Trends in Computing and Communication
ISSN: 2321-8169 Volume: 11 Issue: 10s
DOI: https://doi.org/10.17762/ijritcc.v11i10s.7633
***Article Received:** 02 June 2023 **Revised:** 28 July 2023 **Accepted:** 12 August 2023*

MPAs combine to produce waves that resemble monopoles. The performance other of three MPAs' antennas is excellent.

To address the needs of sub-6 GHz bands coverage and 4x4 MIMO, For 5G terminal applications, [47] discusses a DB FAM Stands for a dual-band 4-antenna module that covers parts of 5G New Radio bands N78 (3.4-3.6 GHz) and N79 (4.8-4.9 GHz). Based on a quarter-circle-shaped dual-mode slotted planar inverted-F antenna (PIFA), TM 11 as well as a hybrid significantly greater mode that integrates quasi-TM 11 and quasi 0,1/2 modes cover the target bands. There are four spinning PIFA components in the four-antenna module. Its diameter is 39.4 mm, and its profile is 1.2 millimeter. The results of the experiments show that the s11 value of the four components contains the preferred frequency band. The isolations between neighbouring elements are greater than 8.5 & 17.6 dB for N78 and 19.4 & 18.5 dB for N79, respectively, the average total efficiencies of the 4 components for N78 are between 38.3 and 39.50 percent, and 39.3 to 42.60 percent for N79, with all envelope correlation coefficients ECC is the lower value of 0.42. Similarly, a Planar H and V-(I.e. Dual) polarized phased array (PD PPA) for 5G wireless communications was investigated by [48]. Wideband, quasi-end-fire, and dual-polarization radiation are printed on a single-layer substrate. Vertically and horizontally polarised components are used on the 5G mobile platform's PCB ground plane. Periodic end-fire slot antennas Both subarrays have a bandwidth of 28-38 GHz (FR-2 5G mmWave bands). The impedance bandwidths of the Co-planar Wave-fed slotted & dipole antennas are 27.1-45.5 GHz and 26.5-395 GHz, respectively. Given a 6-dB(s11) impedance bandwidth, These values may exceed 70 GHz for the slotted antenna & 20 GHz for the dipole antenna. The dual-polarized 5G antenna array has a wide impedance bandwidth, a high realised gain, polarisation, a good radiation pattern, and beam steering. 4.5 mm or less the dual-polarized 5G antenna array clearance, which is sufficient for cellular applications. Thus, it can be observed that existing models vary in terms of their operating characteristics, and internal performance levels. To further evaluate their quantitative performance, the next section compares these models in terms of forward gain levels, bandwidth, complexity of deployment, scalability & cost metrics. This will allow researchers to identify optimum models for the performance-specific use cases.

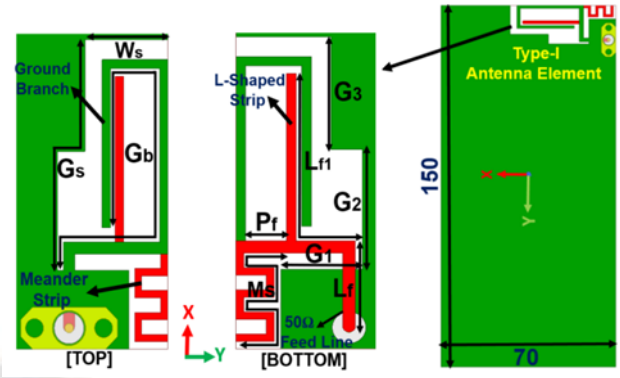

Figure 4. Design of 8-line gain and bandwidth enhancement Antenna of MIMO based-sub 6Ghz frequency [40]

The 3.6 GHz dipole that is the foundation of the antenna's design is supplied by a tapered slot and microstrip line balun. The tapered slot antenna stimulates the dipole at 3.6 GHz, and at 28 GHz, it serves as an antenna. Unique design provides a high-frequency ratio by using a single optimized feeder for both structures.

III. PRAGRAMATIC ANALYSIS & COMPARISON

As per the detailed literature review, it can be observed that existing models showcase high variations in terms of their qualitative characteristics. To further evaluate these models, this section compares them in terms of their Forward Gain Levels (G), Bandwidth (B), Complexity of Deployment (CD), Scalability (S) & Cost (C) Metrics, which will assist researchers to identify optimal models for their deployments. While Gain Levels and bandwidth is directly mentioned by the researchers, levels of deployment complexity, scalability & cost are inferred from internal deployments, and categorized into Low Levels (LL=1), Medium Level (ML=2), High Level (HL=3), and Very High Level (VHL=4), which will assist readers to compare these models on standard scales. This performance can be observed from the following Table 1,

Table 1. Comparative evaluation of different Antennas for 5G Applications

Model	G (dB)	B (GHz)	CD	S	C
LWAUBS [1]	14	24	H	VH	H
DP MPA [2]	5	29	H	VH	H
LPW FCF SPA [3]	8	3.75	VH	L	VH
BWB DPO DA [4]	29	3.22	VH	L	VH
PIFA [5]	10	6	H	M	H
OPA LSC [6]	10	6	M	M	H
PEC TCM [7]	15.4	3.6	M	L	H
DBDP MEDA [8]	14.8	32.2	VH	VH	VH
SIW [9]	10.5	28	H	VH	M

International Journal on Recent and Innovation Trends in Computing and Communication
ISSN: 2321-8169 Volume: 11 Issue: 10s
DOI: https://doi.org/10.17762/ijritcc.v11i10s.7633
***Article Received:** 02 June 2023 **Revised:** 28 July 2023 **Accepted:** 12 August 2023*

HMMP [10]	6	4.6	H	M	H
SRM [11]	16	3.6	H	L	M
MDP BSA [12]	22	4	H	M	H
OMD [13]	21	5	M	M	H
SWP MA [14]	5	6	H	H	H
TS [15]	20	43.9	VH	VH	M
DBDPFA [16]	17.7	5.18	VH	M	H
DBDP MWPA [17]	8	26	H	VH	H
SAPQYA [18]	10	3.8	VH	M	VH
AiPaA [19]	8.3	3.5	H	M	H
FPAR [20]	10.5	5	H	H	M
WCP PAA [21]	19	36.6	VH	VH	H
WISAP [22]	10.8	5	VH	H	VH
HG SAA [23]	19	60	VH	VH	H
Ni EMM [24]	9.6	28	H	VH	H
UC RA [25]	18.9	30	H	VH	H
CA [26]	6.5	28	H	VH	M
WD DAP [27]	15	5	VH	M	H
SIW [28]	10	29.5	H	VH	H
SIT EAA [29]	14.3	3.5	M	L	VH
LPG [30]	4.9	3.1	H	L	H
MLSL SPDT [31]	3	4.1	H	L	H
DPDB NB [32]	6.5	6	M	H	VH
TFC EFA [33]	8.3	8	L	H	H
SGS OE [34]	11	28	M	H	VH
BSF PY [35]	6.2	40	H	VH	VH
FPDP RD ECD [36]	4.8	1.42	VH	L	H
LP WVP MR [37]	6.5	3.8	H	L	VH
TB SA DPA [38]	8.3	2.7	M	L	VH
GCPW [39]	0.46	3.3	H	L	H
UE SGS [40]	20	29	H	VH	VH
DB MM HG SPA [41]	9.1	5.4	H	L	VH
DBSA [42]	10.3	38.5	H	H	H
DPAEFR [43]	9.1	29.5	VH	VH	VH
SPA DP [44]	8.95	4.5	VH	M	H
MAPBEFA [45]	11.6	41	H	VH	VH
YTTW MPA [46]	10.5	4.2	VH	H	VH
DB FAM [47]	19.4	4.9	H	H	H
PD PPA [48]	10	38	M	VH	H

Based on this evaluation, it was observed that BWB DPO DA [4], MDP BSA [12], OMD [13], TS [15], UE SGS [40], DB FAM [47], WCP PAA [21], HG SAA [23], and UC RA [25] showcase higher gain, this can be used for applications that need better signal reproducibility, with minimum errors. Similarly, it was also observed that HG SAA [23], TS [15], MAP BEFA [45], BSF PY [35], DBSA [42], PD PPA [48], WCP PAA [21], DBDP MEDA [8], UC RA [25], SIW [28], DPA EFR [43], DP MPA [2], and UE SGS [40] showcased better bandwidth, thus can be used for high-frequency 5G applications.

It was also observed that TFC EFA [33], OPA LSC [6], PEC TCM [7], OMD [13], SIT EAA [29], DPDB NB [32], SGS OE [34], TB SA DPA [38], and PD PPA [48] showcased lower deployment complexity, thus can be easily deployed for different applications. While, LWA UBS [1], DP MPA [2], DBDP MEDA [8], SIW [9], TS [15], DBDP MWPA [17], WCP PAA [21], HG SAA [23], Ni EMM [24], UC RA [25], CA [26], SIW [28], BSF PY [35], UE SGS [40], DPA EFR [43], MAP BEFA [45], and PD PPA [48] showcased higher scalability levels, thus can be used for large-scale deployment scenarios. It was also evaluated that SIW [9], SRM [11], TS [15], FPAR [20], and CA [26] can be used for low-cost antenna deployment scenarios.

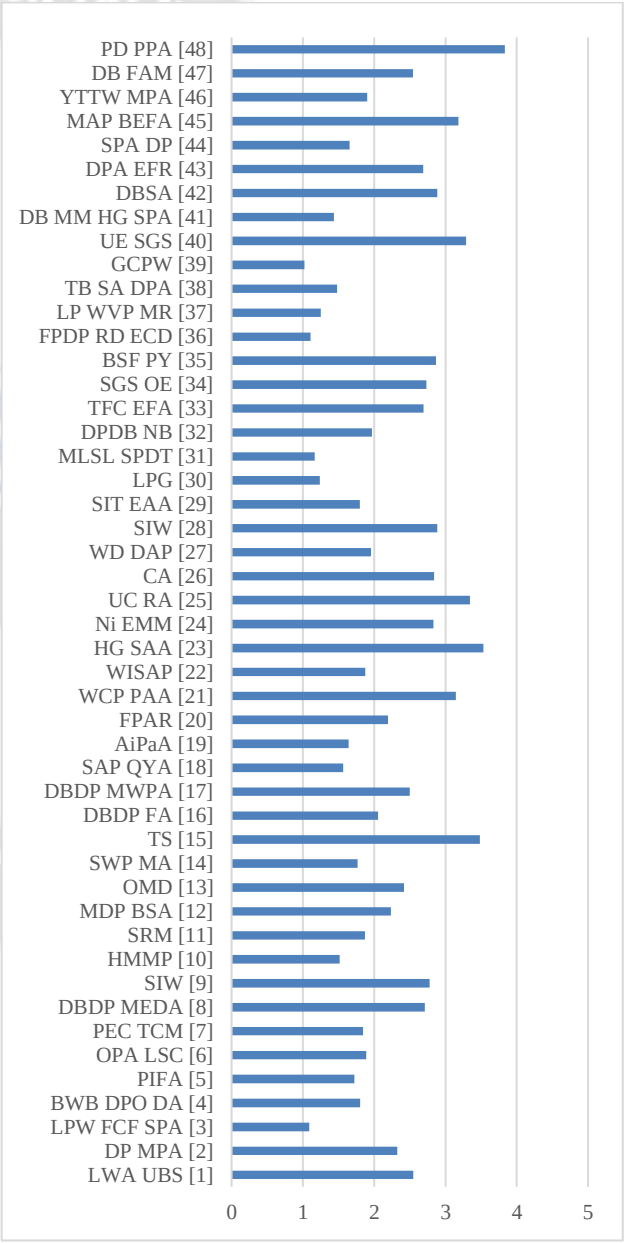

Figure 5. ADRM for different models

International Journal on Recent and Innovation Trends in Computing and Communication
ISSN: 2321-8169 Volume: 11 Issue: 10s
DOI: https://doi.org/10.17762/ijritcc.v11i10s.7633
***Article Received:** 02 June 2023 **Revised:** 28 July 2023 **Accepted:** 12 August 2023*

These performance metrics were combined to form a novel Antenna Design Rank Metric (ADRM) which can be evaluated via equation 1,

ADRM=G/(Max(G))+B/(Max(B))+1/DC+1/C+S/4…(1)

This equation keeps all maximization parameters in numerator, while minimization parameters are kept in the denominator, which assists in identification of models with better overall performance levels. Based on this evaluation and figure 1, it was observed that PD PPA [48], HG SAA [23], TS [15], UC RA [25], UE SGS [40], MAP BEFA [45], WCP PAA [21], DBSA [42], SIW [28], BSF PY [35], CA [26], and Ni EMM [24] showcase higher gain, with higher bandwidth & better scalability, along with lower complexity & lower cost, thus can be used for a wide variety of use cases.

IV. CONCLUSION AND FUTURE SCOPE

This extensive review explains multiple antenna design models and discusses their performance in terms of different qualitative & quantitate metrics. Based on this evaluation, it was observed that Yagi Antennas, Polarized Phased Array Antennas, Superstrate Antenna Array, and Square Ground Slot type antennas provide better performance levels. It was also discovered that BWB DPO DA, MDP BSA, OMD, TS, UE SGS, DB FAM, WCP PAA, HG SAA, and UC RA had a greater gain. This quality may be put to use in software programs that need improved signal repeatability while minimizing the number of mistakes that occur. In a similar vein, it was shown that HG SAA, TS, MAP BEFA, BSF PY, DBSA, PD PPA, WCP PAA, DBDP MEDA, UC RA, SIW, DPA EFR, DP MPA, and UE SGS all exhibited improved bandwidth, and as a result, they are all suitable for use in high-frequency G applications. TFC EFA, OPA LSC, PEC TCM, OMD, SIT EAA, DPDB NB, SGS OE, TB SA DPA, and PD PPA all shown decreased deployment complexity, and as a result, they are more readily adaptable to a variety of applications. While other protocols, such as LWA UBS, DP MPA, DBDP MEDA, SIW, TS, DBDP MWPA, WCP PAA, HG SAA, Ni EMM, UC RA, CA, SIW, BSF PY, UE SGS, DPA EFR, MAP BEFA, and PD PPA, shown better degrees of scalability and are hence suitable for usage in large-scale deployment situations, It was also determined that SIW, SRM, TS, FPAR, and CA are all capable of being used in situations involving low-cost antenna placement. On the basis of the novel Antenna Design Rank Metric, it was observed that PD PPA, HG SAA, TS, UC RA, UE SGS, MAP BEFA, WCP PAA, DBSA, SIW, BSF PY, CA, and Ni EMM showcase higher gain, with higher bandwidth and better scalability, along with lower complexity and lower cost, and therefore can be used for a wide variety of use cases. In future, researchers can combine these models to generate better antenna designs, polarity & gain levels can also be improved via fusion techniques. Moreover, higher frequency antennas can be combined with lower frequency antennas via bioinspired computing to improve gain levels while maintaining lower cost, lower complexity, and higher scalability levels under different scenarios.

ACKNOWLEDGEMENT

I am grateful to Dr. N. V. Rajasekhar, my guide, for all of his help in gathering information and arranging it into useful formats, and to VIT-AP UNIVERSITY for allowing me to use their resources.

REFERENCES

[1] A. Goudarzi, M. M. Honari and R. Mirzavand, "A Millimeter-Wave Fabry–Perot Cavity Antenna With Unidirectional Beam Scanning Capability for 5G Applications," in IEEE Transactions on Antennas and Propagation, vol. 70, no. 3, pp. 1787-1796, March 2022, doi: 10.1109/TAP.2021.3118796

[2] G. Kim and S. Kim, "Design and Analysis of Dual Polarized Broadband Microstrip Patch Antenna for 5G mmWave Antenna Module on FR4 Substrate," in IEEE Access, vol. 9, pp. 64306-64316, 2021, doi: 10.1109/ACCESS.2021.3075495.

[3] K. -L. Wong, M. -F. Jian and W. -Y. Li, "Low-Profile Wideband Four-Corner-Fed Square Patch Antenna for 5G MIMO Mobile Antenna Application," in IEEE Antennas and Wireless Propagation Letters, vol. 20, no. 12, pp. 2554-2558, Dec. 2021, doi: 10.1109/LAWP.2021.3119753.

[4] Y. Feng, F. -S. Zhang, G. -J. Xie, Y. Guan and J. Tian, "A Broadband and Wide-Beamwidth Dual-Polarized Orthogonal Dipole Antenna for 4G/5G Communication," in IEEE Antennas and Wireless Propagation Letters, vol. 20, no. 7, pp. 1165-1169, July 2021, doi: 10.1109/LAWP.2021.3074558.

[5] X. -T. Yuan, Z. Chen, T. Gu and T. Yuan, "A Wideband PIFA-Pair-Based MIMO Antenna for 5G Smartphones," in IEEE Antennas and Wireless Propagation Letters, vol. 20, no. 3, pp. 371-375, March 2021, doi: 10.1109/LAWP.2021.3050337.

[6] D. Serghiou, M. Khalily, V. Singh, A. Araghi and R. Tafazolli, "Sub-6 GHz Dual-Band 8 × 8 MIMO Antenna for 5G Smartphones," in IEEE Antennas and Wireless Propagation Letters, vol. 19, no. 9, pp. 1546-1550, Sept. 2020, doi: 10.1109/LAWP.2020.3008962.

[7] H. H. Zhang, X. Z. Liu, G. S. Cheng, Y. Liu, G. M. Shi and K. Li, "Low-SAR Four-Antenna MIMO Array for 5G Mobile Phones Based on the Theory of Characteristic Modes of Composite PEC-Lossy Dielectric Structures," in IEEE Transactions on Antennas and Propagation, vol. 70, no. 3, pp. 1623-1631, March 2022, doi: 10.1109/TAP.2021.3133432.

[8] Y. Cheng and Y. Dong, "Dual-Broadband Dual-Polarized Shared-Aperture Magnetoelectric Dipole Antenna for 5G Applications," in IEEE Transactions on Antennas and Propagation, vol. 69, no. 11, pp. 7918-7923, Nov. 2021, doi: 10.1109/TAP.2021.3083744.

[9] J. Puskely, T. Mikulasek, Y. Aslan, A. Roederer and A. Yarovoy, "5G SIW-Based Phased Antenna Array With Cosecant-Squared Shaped Pattern," in IEEE Transactions on Antennas and Propagation, vol. 70, no. 1, pp. 250-259, Jan. 2022, doi: 10.1109/TAP.2021.3098577.

International Journal on Recent and Innovation Trends in Computing and Communication
ISSN: 2321-8169 Volume: 11 Issue: 10s
DOI: https://doi.org/10.17762/ijritcc.v11i10s.7633
***Article Received:** 02 June 2023 **Revised:** 28 July 2023 **Accepted:** 12 August 2023*

[10] L. Chang, G. Zhang and H. Wang, "Triple-Band Microstrip Patch Antenna and its Four-Antenna Module Based on Half-Mode Patch for 5G 4 × 4 MIMO Operation," in IEEE Transactions on Antennas and Propagation, vol. 70, no. 1, pp. 67-74, Jan. 2022, doi: 10.1109/TAP.2021.3090572.

[11] H. H. Zhang et al., "Low-SAR MIMO Antenna Array Design Using Characteristic Modes for 5G Mobile Phones," in IEEE Transactions on Antennas and Propagation, vol. 70, no. 4, pp. 3052-3057, April 2022, doi: 10.1109/TAP.2021.3121174.

[12] K. Xue, D. Yang, C. Guo, H. Zhai, H. Li and Y. Zeng, "A Dual-Polarized Filtering Base-Station Antenna With Compact Size for 5G Applications," in IEEE Antennas and Wireless Propagation Letters, vol. 19, no. 8, pp. 1316-1320, Aug. 2020, doi: 10.1109/LAWP.2020.2998871.

[13] L. Sun, Y. Li, Z. Zhang and Z. Feng, "Wideband 5G MIMO Antenna With Integrated Orthogonal-Mode Dual-Antenna Pairs for Metal-Rimmed Smartphones," in IEEE Transactions on Antennas and Propagation, vol. 68, no. 4, pp. 2494-2503, April 2020, doi: 10.1109/TAP.2019.2948707.

[14] X. Gu et al., "Antenna-in-Package Integration for a Wideband Scalable 5G Millimeter-Wave Phased-Array Module," in IEEE Microwave and Wireless Components Letters, vol. 31, no. 6, pp. 682-684, June 2021, doi: 10.1109/LMWC.2021.3071917.

[15] H. Chen, Y. Tsai, C. Sim and C. Kuo, "Broadband Eight-Antenna Array Design for Sub-6 GHz 5G NR Bands Metal-Frame Smartphone Applications," in IEEE Antennas and Wireless Propagation Letters, vol. 19, no. 7, pp. 1078-1082, July 2020, doi: 10.1109/LAWP.2020.2988898.

[16] Y. Li, Z. Zhao, Z. Tang and Y. Yin, "Differentially Fed, Dual-Band Dual-Polarized Filtering Antenna With High Selectivity for 5G Sub-6 GHz Base Station Applications," in IEEE Transactions on Antennas and Propagation, vol. 68, no. 4, pp. 3231-3236, April 2020, doi: 10.1109/TAP.2019.2957720.

[17] Y. He, S. Lv, L. Zhao, G. -L. Huang, X. Chen and W. Lin, "A Compact Dual-Band and Dual-Polarized Millimeter-Wave Beam Scanning Antenna Array for 5G Mobile Terminals," in IEEE Access, vol. 9, pp. 109042-109052, 2021, doi: 10.1109/ACCESS.2021.3100933.

[18] Z. Wang, Y. Ning and Y. Dong, "Compact Shared Aperture Quasi-Yagi Antenna With Pattern Diversity for 5G-NR Applications," in IEEE Transactions on Antennas and Propagation, vol. 69, no. 7, pp. 4178-4183, July 2021, doi: 10.1109/TAP.2020.3044633.

[19] H. -C. Huang and J. Lu, "Evolution of Innovative 5G Millimeter-Wave Antenna Designs Integrating Non-Millimeter-Wave Antenna Functions Based on Antenna-in-Package (AiP) Solution to Cellular Phones," in IEEE Access, vol. 9, pp. 72516-72523, 2021, doi: 10.1109/ACCESS.2021.3077309.

[20] K. -L. Wong, J. -Z. Chen and W. -Y. Li, "Four-Port Wideband Annular-Ring Patch Antenna Generating Four Decoupled Waves for 5G Multi-Input–Multi-Output Access Points," in IEEE Transactions on Antennas and Propagation, vol. 69, no. 5, pp. 2946-2951, May 2021, doi: 10.1109/TAP.2020.3025237.

[21] Y. Cheng and Y. Dong, "Wideband Circularly Polarized Planar Antenna Array for 5G Millimeter-Wave Applications," in IEEE Transactions on Antennas and Propagation, vol. 69, no. 5, pp. 2615-2627, May 2021, doi: 10.1109/TAP.2020.3028213.

[22] L. Sun, Y. Li and Z. Zhang, "Wideband Decoupling of Integrated Slot Antenna Pairs for 5G Smartphones," in IEEE Transactions on Antennas and Propagation, vol. 69, no. 4, pp. 2386-2391, April 2021, doi: 10.1109/TAP.2020.3021785.

[23] Y. Al-Alem and A. A. Kishk, "Low-Cost High-Gain Superstrate Antenna Array for 5G Applications," in IEEE Antennas and Wireless Propagation Letters, vol. 19, no. 11, pp. 1920-1923, Nov. 2020, doi: 10.1109/LAWP.2020.2974455.

[24] H. Qiu et al., "Compact, Flexible, and Transparent Antennas Based on Embedded Metallic Mesh for Wearable Devices in 5G Wireless Network," in IEEE Transactions on Antennas and Propagation, vol. 69, no. 4, pp. 1864-1873, April 2021, doi: 10.1109/TAP.2020.3035911.

[25] P. Mei, S. Zhang and G. F. Pedersen, "A Low-Cost, High-Efficiency and Full-Metal Reflectarray Antenna With Mechanically 2-D Beam-Steerable Capabilities for 5G Applications," in IEEE Transactions on Antennas and Propagation, vol. 68, no. 10, pp. 6997-7006, Oct. 2020, doi: 10.1109/TAP.2020.2993077.

[26] M. Ikram, N. Nguyen-Trong and A. M. Abbosh, "Common-Aperture Sub-6 GHz and Millimeter-Wave 5G Antenna System," in IEEE Access, vol. 8, pp. 199415-199423, 2020, doi: 10.1109/ACCESS.2020.3034887.

[27] Y. Q. Hei, J. G. He and W. T. Li, "Wideband Decoupled 8-Element MIMO Antenna for 5G Mobile Terminal Applications," in IEEE Antennas and Wireless Propagation Letters, vol. 20, no. 8, pp. 1448-1452, Aug. 2021, doi: 10.1109/LAWP.2021.3086261.

[28] H. Li, Y. Li, L. Chang, W. Sun, X. Qin and H. Wang, "A Wideband Dual-Polarized Endfire Antenna Array With Overlapped Apertures and Small Clearance for 5G Millimeter-Wave Applications," in IEEE Transactions on Antennas and Propagation, vol. 69, no. 2, pp. 815-824, Feb. 2021, doi: 10.1109/TAP.2020.3016512.

[29] S. S. Alja'afreh et al., "Ten Antenna Array Using a Small Footprint Capacitive-Coupled-Shorted Loop Antenna for 3.5 GHz 5G Smartphone Applications," in IEEE Access, vol. 9, pp. 33796-33810, 2021, doi: 10.1109/ACCESS.2021.3061640.

[30] S. Youn, D. Jang, N. K. Kong and H. Choo, "Design of a Printed 5G Monopole Antenna With Periodic Patch Director on the Laminated Window Glass," in IEEE Antennas and Wireless Propagation Letters, vol. 21, no. 2, pp. 297-301, Feb. 2022, doi: 10.1109/LAWP.2021.3128648.

[31] K. Trzebiatowski, M. Rzymowski, L. Kulas and K. Nyka, "Simple 60 GHz Switched Beam Antenna for 5G Millimeter-Wave Applications," in IEEE Antennas and Wireless Propagation Letters, vol. 20, no. 1, pp. 38-42, Jan. 2021, doi: 10.1109/LAWP.2020.3038260.

[32] Z. Li, J. Han, Y. Mu, X. Gao and L. Li, "Dual-Band Dual-Polarized Base Station Antenna With a Notch Band for 2/3/4/5G Communication Systems," in IEEE Antennas and Wireless Propagation Letters, vol. 19, no. 12, pp. 2462-2466, Dec. 2020, doi: 10.1109/LAWP.2020.3035559.

[33] H. Kim and S. Nam, "Performance Enhancement of 5G Millimeter Wave Antenna Module Integrated Tablet Device," in IEEE Transactions on Antennas and Propagation, vol. 69, no. 7, pp. 3800-3810, July 2021, doi: 10.1109/TAP.2020.3044651.

International Journal on Recent and Innovation Trends in Computing and Communication
ISSN: 2321-8169 Volume: 11 Issue: 10s
DOI: https://doi.org/10.17762/ijritcc.v11i10s.7633
***Article Received:** 02 June 2023 **Revised:** 28 July 2023 **Accepted:** 12 August 2023*

[34] M. Ikram, N. Nguyen-Trong and A. Abbosh, "Hybrid Antenna Using Open-Ended Slot for Integrated 4G/5G Mobile Application," in IEEE Antennas and Wireless Propagation Letters, vol. 19, no. 4, pp. 710-714, April 2020, doi: 10.1109/LAWP.2020.2978181.

[35] Salim G. Shaikh, B. Suresh Kumar, Geetika Narang, & N.N.Pachpor. (2023). Diagnosis of Vector Borne Disease using Various Machine Learning Techniques. International Journal of Intelligent Systems and Applications in Engineering, 11(4s), 517–526. Retrieved from https://ijisae.org/index.php/IJISAE/article/view/2721

[36] T. -H. Lin et al., "Broadband and Miniaturized Antenna-in-Package (AiP) Design for 5G Applications," in IEEE Antennas and Wireless Propagation Letters, vol. 19, no. 11, pp. 1963-1967, Nov. 2020, doi: 10.1109/LAWP.2020.3018064.

[37] S. Martin-Anton and D. Segovia-Vargas, "Fully Planar Dual-Polarized Broadband Antenna for 3G, 4G and Sub 6-GHz 5G Base Stations," in IEEE Access, vol. 8, pp. 91940-91947, 2020, doi: 10.1109/ACCESS.2020.2994382.

[38] S. Wen and Y. Dong, "A Low-Profile Wideband Antenna With Monopolelike Radiation Characteristics for 4G/5G Indoor Micro Base Station Application," in IEEE Antennas and Wireless Propagation Letters, vol. 19, no. 12, pp. 2305-2309, Dec. 2020, doi: 10.1109/LAWP.2020.3030968.

[39] D. He, Y. Chen and S. Yang, "A Low-Profile Triple-Band Shared-Aperture Antenna Array for 5G Base Station Applications," in IEEE Transactions on Antennas and Propagation, vol. 70, no. 4, pp. 2732-2739, April 2022, doi: 10.1109/TAP.2021.3137486.

[40] R. R. Barani, K. Wong, Y. Zhang and W. Li, "Low-Profile Wideband Conjoined Open-Slot Antennas Fed by Grounded Coplanar Waveguides for $4\times4\,\,5$ G MIMO Operation," in IEEE Transactions on Antennas and Propagation, vol. 68, no. 4, pp. 2646-2657, April 2020, doi: 10.1109/TAP.2019.2957967.

[41] S. P. Biswal, S. K. Sharma and S. Das, "Collocated Microstrip Slot MIMO Antennas for Cellular Bands Along With 5G Phased Array Antenna for User Equipments (UEs)," in IEEE Access, vol. 8, pp. 209138-209152, 2020, doi: 10.1109/ACCESS.2020.3038328.

[42] J. Hao, N. Yan, Y. Luo, H. Fu and K. Ma, "A Low-Cost Dual-Band Multimode High-Gain Stacked-Patch Antenna Based on SISL for 5G Applications," in IEEE Antennas and Wireless Propagation Letters, vol. 21, no. 1, pp. 4-8, Jan. 2022, doi: 10.1109/LAWP.2021.3112459.

[43] J. Hwang, J. -I. Oh, H. -W. Jo, K. -S. Kim, J. -W. Yu and D. -J. Lee, "28 GHz and 38 GHz Dual-Band Vertically Stacked Dipole Antennas on Flexible Liquid Crystal Polymer Substrates for Millimeter-Wave 5G Cellular Handsets," in IEEE Transactions on Antennas and Propagation, vol. 70, no. 5, pp. 3223-3236, May 2022, doi: 10.1109/TAP.2021.3137234.

[44] M. Faizi Khajeim, G. Moradi, R. Sarraf Shirazi and S. Zhang, "Broadband Dual-Polarized Antenna Array With Endfire Radiation for 5G Mobile Phone Applications," in IEEE Antennas and Wireless Propagation Letters, vol. 20, no. 12, pp. 2427-2431, Dec. 2021, doi: 10.1109/LAWP.2021.3113993.

[45] M. Ciydem and E. A. Miran, "Dual-Polarization Wideband Sub-6 GHz Suspended Patch Antenna for 5G Base Station," in IEEE Antennas and Wireless Propagation Letters, vol. 19, no. 7, pp. 1142-1146, July 2020, doi: 10.1109/LAWP.2020.2991967.

[46] J. Seo et al., "Miniaturized Dual-Band Broadside/Endfire Antenna-in-Package for 5G Smartphone," in IEEE Transactions on Antennas and Propagation, vol. 69, no. 12, pp. 8100-8114, Dec. 2021, doi: 10.1109/TAP.2021.3088230.

[47] K. Wong, H. Chang, J. Chen and K. Wang, "Three Wideband Monopolar Patch Antennas in a Y-Shape Structure for 5G Multi-Input–Multi-Output Access Points," in IEEE Antennas and Wireless Propagation Letters, vol. 19, no. 3, pp. 393-397, March 2020, doi: 10.1109/LAWP.2020.2967354.

[48] Kevin Harris, Lee Green, Juan González, Juan Garciam, Carlos Rodríguez. Automated Content Generation for Personalized Learning using Machine Learning. Kuwait Journal of Machine Learning, 2(2). Retrieved from http://kuwaitjournals.com/index.php/kjml/article/view/180

[49] L. Chang and H. Wang, "Dual-Band Four-Antenna Module Covering N78/N79 Based on PIFA for 5G Terminals," in IEEE Antennas and Wireless Propagation Letters, vol. 21, no. 1, pp. 168-172, Jan. 2022, doi: 10.1109/LAWP.2021.3122425.

[50] N. O. Parchin, J. Zhang, R. A. Abd-Alhameed, G. F. Pedersen and S. Zhang,"A Planar Dual-Polarized Phased Array With Broad Bandwidth and Quasi-Endfire Radiation for 5G Mobile Handsets," in IEEE Transactions on Antennas and Propagation, vol. 69, no. 10, pp. 6410-6419, Oct. 2021, doi: 10.1109/TAP.2021.3069501.